Supporting Information

Lukaszewicz and Anderson 10.1073/pnas.1106230108

SI Text 1

Modeling GOF Electroporation. We tested whether mD1KE overexpression could lead indirectly to an increase in the size of the neurogenic ($Lim3^+$) population in the pMN domain, by selectively decreasing the relative size of the nonneurogenic ($Lim3^-$) population. Our failure to detect an increase in activated caspase-3 expression caused by mD1KE overexpression excludes a role for selective cell death. Therefore, here we consider only the possibility that mD1KE overexpression selectively inhibits the proliferation of the nonneurogenic subpopulation of $Olig2^+$ cells, thereby indirectly increasing the relative size of the neurogenic subpopulation.

Observed values from overexpressing mD1KE at cE2 and analyzing on cE4 included the following:

A 35.8% increase in the $Lim3^+$ population with the pMN domain
An 8.5% increase in the LI (LI = %$BrdU^+$ among $Olig2^+$ cells)
A 9.25% decrease in the pMN size (#$Olig2^+$ total).

In the control pMN at cE4, ~30% of $Olig2^+$ cells are $Lim3^+$. In the calculation that follows, for illustrative purposes we assume a total $Olig2^+$ population size of 100 cells. If so, then, based on our measurements, the cE4 $Olig2^+$ population would consist of 30 $Lim3^+$ cells and 70 $Lim3^-$ cells.

mD1KE overexpression causes a 35.8% increase in the percentage of $Olig2^+$ cells that are $Lim3^+$. According to the alternative hypothesis investigated here, this increase would be indirectly due to a selective *decrease* in the size of the $Lim3^-$ $Olig2^+$ cell population. If so, then to produce a 35.8% increase in the percentage of $Lim3^+$ $Olig2^+$ cells in the pMN domain, mD1KE overexpression would have to reduce the absolute number of $Lim3^-$ $Olig2^+$ cells from 70 to ~43.6 (in the example of 100 total $Olig2^+$ cells). Such a decrease implies that the overall size of the pMN domain should drop from 100 cells (30 $Lim3^+$ + 70 $Lim3^-$) to 73.6 (30 + 43.6), a 26.3% reduction. However, our cell counts indicate that overexpression of mD1KE caused only a 9.2% reduction in the total number of $Olig2^+$ cells.

Furthermore, this explanation is also inconsistent with the results of our BrdU labeling experiments. According to the model, the ~36% increase in the size of the $Lim3^+$ subpopulation of $Olig2^+$ cells would actually be due to an ~37.7% decrease in the size of the $Lim3^-$ subpopulation (from 70 to 43.6 cells in this example). If this reduction is not due to selective cell death (see above), then it must reflect a cell cycle kinetic slowdown during the 36-h period when mD1KE is expressed efficiently.

To investigate this possibility, we calculated the number of cell cycles that a spinal cord progenitor cell could undergo during the 36-h period between electroporation and analysis. The average duration of the S phase (*Ts*) is 4.5 h in the chicken embryonic optic tectum (2). With Ts being constant (2, 3), we used this value to calculate the cell cycle duration (*Tc*) in the pMN domain of the spinal cord. In control embryos, the LI measured in BrdU pulse-labeling experiments was ~28%. Within the growth fraction, the LI equals *Ts*/*Tc* (4). Thus, given *Ts* and a measured LI of 28%, *Tc* can be calculated as 4.5/0.28 = 16 h/cell cycle. This cell cycle duration is comparable to that measured by others in the developing chick spinal cord (5). This value of *Tc* indicates that during our 36-h experiment, $Olig2^+$ cells in control embryos have time to go through 2.25 cell cycles (36/16). Therefore, assuming that all $Olig2^+$ cells undergo symmetric proliferative divisions during this interval, the 70 $Olig2^+$ $Lim3^-$ cells present at cE4 must have derived from 14.7 cells [70/2exp(2.25)] present 36 h earlier.

Now, under the conditions of mD1KE overexpression, if those 14.7 cells at cE2.5 gave rise to only 43.2 cells at cE4, it would mean that they accomplished only 1.47 cell cycles, instead of 2.25 cycles, in 36 h. If so, then, because *Ts* is constant, *Tc* would have to be increased to 24.5 h.

If mD1KE overexpression indeed selectively slowed the cell cycle time of $Lim3^-$ cells from 16 to 24.5 h/cell cycle, then the predicted LI of the $Lim3^-$ subpopulation of $Olig2^+$ cells in mD1KE-electroporated embryos should be *Ts*/*Tc* = 4.5/24.5 = 18.4%. This corresponds to a 34% reduction in the LI of this $Lim3^-$ $Olig2^+$ cell subpopulation compared with control embryos (LI = 28%). Instead, we observe an 8.5% *increase* in the LI of $Olig2^+$ cells after mD1KE electroporation.

These two inconsistencies argue against a model in which mD1KE indirectly increases the proportion of the $Lim3^+$ $Olig2^+$ cell population by selectively slowing the proliferation of the $Lim3^-$ subpopulation.

Modeling cD1 siRNA Electroporation. We also tested whether cD1 knockdown could lead indirectly to a decrease in the size of the neurogenic ($Lim3^+$) population in the pMN domain, by selectively increasing the relative size of the nonneurogenic ($Lim3^-$) population through an effect on proliferation. Observed values after the down-regulation of cD1 from cE2 to cE4 included the following:

- A 28.1% decrease in the $Lim3^+$ population with the pMN domain
- A 28.2% decrease in the LI (LI = %$BrdU^+$ among $Olig2^+$ total)
- A 43.3% decrease in the pMN size (#$Olig2^+$ total).

Here again, for illustrative purposes we assume a total $Olig2^+$ population of 100 cells in control embryos at cE4, of which 30% are $Lim3^+$ and 70% are $Lim3^-$.

cD1siRNA causes a 28.1% decrease in the percentage of $Olig2^+$ cells that are $Lim3^+$. If, according to this model, this decrease were due exclusively to an increase in the size of the $Lim3^-$ $Olig2^+$ population, then (in the current example) the pMN domain of such embryos would be composed of 30 $Lim3^+$ cells and 109 $Lim3^-$ cells (a 28.1% decrease). In other words, the size of the $Lim3^-$ population would have to increase by 56% (from 70 to 109 cells). This implies that the overall size of the pMN domain should increase by 39% after cD1 knockdown, from 100 (30 + 70) to 139 (30 + 109). Instead, we observe a 43.3% reduction in the total number of $Olig2^+$ cells caused by this manipulation.

This difference notwithstanding, how much of an increase in proliferation rate would be required to produce a 56% increase in the size of the $Olig2^+$ $Lim3^-$ population? If, after cD1 knockdown, the 14.7 $Lim3^-$ cells present at the time of electroporation (E2.5) give rise to 109 cells 36 h later, at cE4, that means that they accomplished 2.85 cycles in 36 h; thus *Tc* = 12.6 h. The LI should then be *Ts*/*Tc* = 4.5/12.6 = 35.7%. This corresponds to a predicted 27.5% increase in the LI of $Lim3^-$ $Olig2^+$ cells compared with control embryos (LI = 28%). Instead, we observe a 28.2% reduction in the LI of the entire $Olig2^+$ cells. These inconsistencies between prediction and observation argue against a selective increase in the proliferation of nonneurogenic $Olig2^+$ cells as an explanation for the decrease in the proportion of neurogenic cells caused by cD1 knockdown.

SI Text 2

The effect of cD1 knockdown in decreasing the expression level of Hes6 (but not Hes5) suggests that Cyclin D1 expression is required, either directly or indirectly, for Hes6 expression (Fig. 3). However, we did not observe a measureable increase in Hes6 mRNA by in situ hybridization after Cyclin D1 overexpression. Several explanations may account for this apparent discrepancy:

1. Cyclin D1 could control Hes6 expression in a permissive manner. In this model, Cyclin D1 controls *Hes6* gene expression in a manner that is necessary but not sufficient.
2. The decrease in *Hes6* expression observed after cD1 down-regulation reflects the death of Hes6-expressing cells, rather than a loss of Hes6 expression. Overexpression of mD1 does not increase the survival of these cells, because there is little ongoing cell death. We did not observe any significant increase in the number of cells expressing activated caspase-3 after cD1 knockdown, arguing against this hypothesis. Nevertheless, we cannot exclude the possibility that cell death that was rapidly cleared was missed by our analysis.
3. The down-regulation of cD1 could prevent the formation of Hes6-expressing cells, leading to an overall decrease in the level of Hes6 expression. However, this explanation is inconsistent with the fact that overexpression of mD1 increases neuronal production, which should be marked by Hes6 up-regulation. As discussed in the second part of *Discussion*, it is possible that the small (~20%) increase in the number of neuronal progenitor cells caused by mD1 overexpression, which is measured by counting individual antibody-stained nuclei, is too small to be detected by our in situ hybridization method, which does not have cellular resolution.
4. Overexpression of mD1 does increase the level of Hes6, inducing neuronal specification, but its proliferation-stimulating effect simultaneously increases (directly or indirectly) Hes5 expression. If Hes5 suppresses expression of Hes6, then the two effects of Cyclin D1 could cancel out each other. However, we did not observe any increase in Hes6 expression when the cell cycle mutant mD1KE was overexpressed, although this failure is subject to the same caveat regarding the sensitivity of our in situ hybridization method (see item 3).
5. The Hes6-expressing population could be a transient intermediate population that rapidly differentiates into neurons. In this case, the rate of differentiation of $Hes6^+$ progenitors is not limiting. $Hes6^+$ precursors immediately differentiate into postmitotic neurons and migrate away from the VZ. Therefore, increasing the production of these cells by mD1 overexpression does not result in a measureable increase in the steady-sate number of $Hes6^+$ cells (and thus in the level of Hes6 expression).

SI Materials and Methods

The following antibodies were used: AMV (mouse monoclonal; Developmental Studies Hybridoma Bank), BrdU (rat monoclonal; Abcam), mono-β-tubulin (Tuj1, mouse monoclonal; Covance), activated caspase-3 (rabbit polyclonal; R&D Systems), Cyclin D1 (mouse monoclonal 72-13G; Santa Cruz Biotechnology or rabbit monoclonal SP4; Thermo Scientific), Cyclin D2 (rabbit polyclonal M-20; Santa Cruz Biotechnology), Engrail-1 (mouse monoclonal; Developmental Studies Hybridoma Bank), GFP (chicken polyclonal; Abcam), GFP (rabbit polyclonal; Molecular Probes), HB9 (mouse monoclonal MNR2; Developmental Studies Hybridoma Bank), Lim3/Lhx3 (rabbit polyclonal, a gift from T. Jessell, Columbia University), mNeuN (mouse monoclonal MAB377; Chemicon), NeuroM (rat polyclonal, a gift from B. Novitch, University of California, Los Angeles), mNgn2 (mouse monoclonal, provided by D.J.A.), hOlig2 (goat polyclonal; R&D Systems), Olig2 (rabbit polyclonal DF308, a gift from D. Rowitch, University of California, San Francisco), PCNA (mouse monoclonal MAB424; Chemicon), and QCPN (mouse monoclonal; Developmental Studies Hybridoma Bank).

1. Lobjois V, Bel-Vialar S, Trousse F, Pituello F (2008) Forcing neural progenitor cells to cycle is insufficient to alter cell-fate decision and timing of neuronal differentiation in the spinal cord. *Neural Dev* 3:4.
2. Wilson DB (1973) Chronological changes in the cell cycle of chick neuroepithelial cells. *J Embryol Exp Morphol* 29:745–751.
3. Caviness VSJ, Jr., Takahashi T, Nowakowski RS (1995) Numbers, time and neocortical neuronogenesis: A general developmental and evolutionary model. *Trends Neurosci* 18:379–383.
4. Nowakowski RS, Lewin SB, Miller MW (1989) Bromodeoxyuridine immunohistochemical determination of the lengths of the cell cycle and the DNA-synthetic phase for an anatomically defined population. *J Neurocytol* 18:311–318.
5. Wilcock AC, Swedlow JR, Storey KG (2007) Mitotic spindle orientation distinguishes stem cell and terminal modes of neuron production in the early spinal cord. *Development* 134:1943–1954.

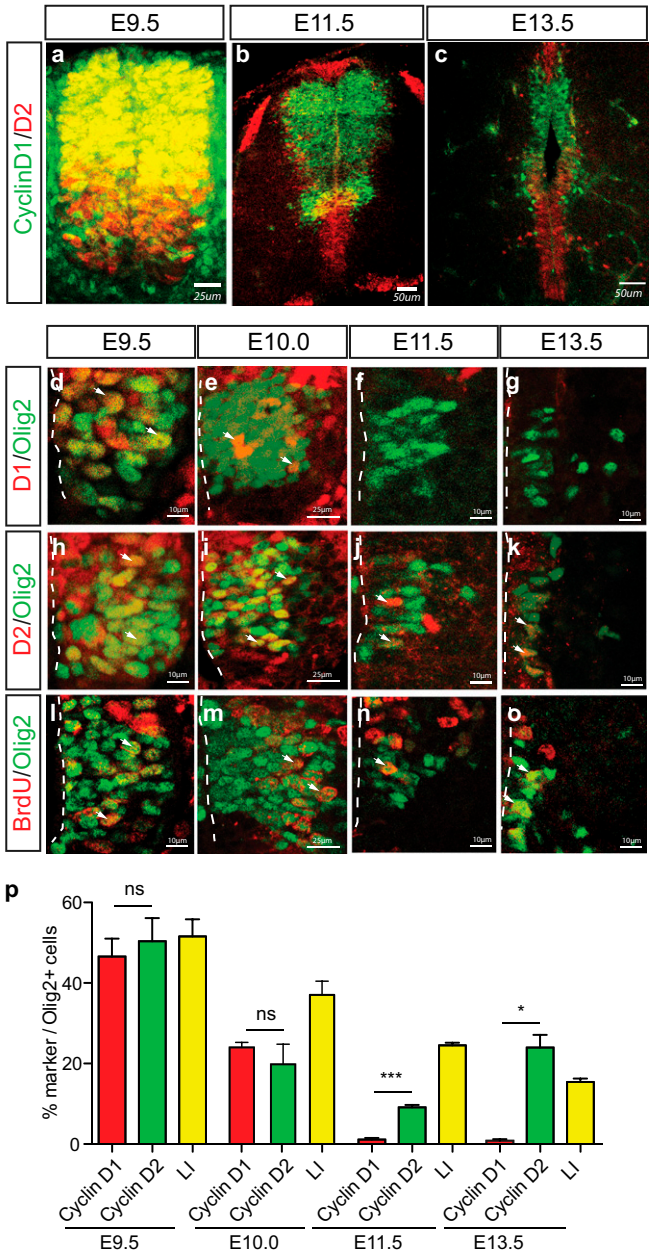

Fig. S1. Extinction of Cyclin D1 expression correlates with loss of neurogenic potential during the switch to gliogenesis. (*A*–*C*) Double-immunolabeling for Cyclin D1 and D2 in the whole spinal cord at E19.5, E11.5, and E13.5. Cyclin D1 and D2 are coexpressed at early stages (*A*), but Cyclin D1 expression became progressively *restricted* to the dorsal region with further development (*B* and *C*). (*D*–*O*) Double-immunostaining for Olig2 and Cyclin D1 (*D*–*G*), D2 (*H*–*K*), or BrdU (*L*–*O*) at the indicated days of mouse development. Dashed lines indicate the midline. Arrowheads indicate double-positive cells. (P) Quantification of the percentage of Olig2$^+$ cells expressing Cyclin D1 D2, or BrdU at the indicated days of mouse development. Values are mean ± SEM of between four and six sections from between three and six embryos. *$P < 0.05$; **$P < 0.01$; ***$P < 0.001$ (*t* test).

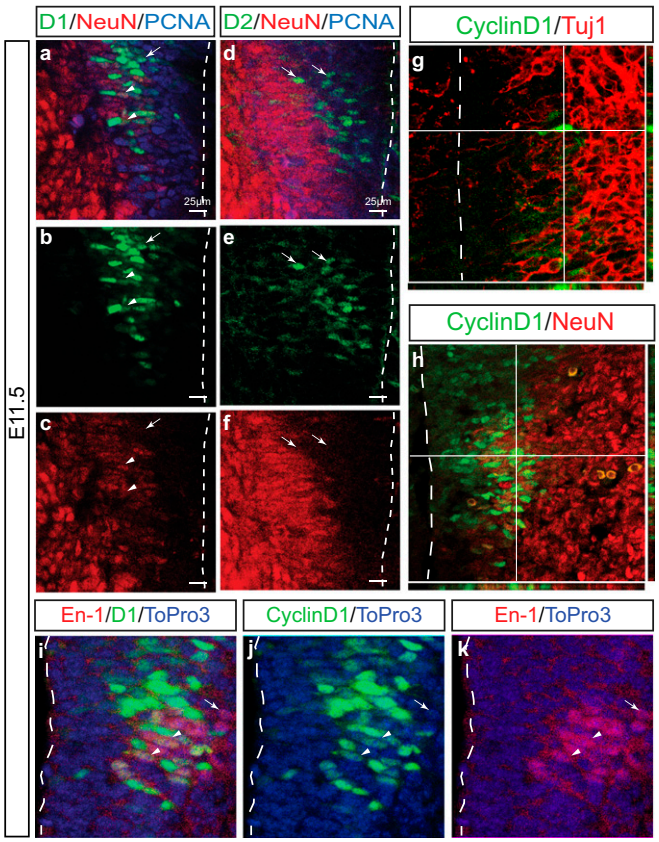

Fig. S2. Cyclin D1 expression persists in newly-born neurons. To confirm Cyclin D1 expression in newly postmitotic neurons, we analyzed its expression in the E11.5 spinal cord. Whereas all Cyclin D2-expressing nuclei are confined to the PCNA$^+$ VZ (*D–F*), some Cyclin D1$^+$ cells were adjacent to the core of the VZ (*A–C*). These Cyclin D1$^+$ nuclei have down-regulated PCNA (*A–C*), and some express NeuN (*A–C*, *H*) or Tuj1 (*G*). This result suggests that they are newly postmitotic neurons migrating away from the VZ. Some Cyclin D1$^+$ neurons can be identified as V1 interneurons, based on their expression of Engrailed 1 (*I–K*); 62.2% (n = 3 $\pm$ 5.8) of E11.5 Engrailed1$^+$ neurons express Cyclin D1, whereas virtually none of them express Cyclin D2 (3.05% $\pm$ 0.626%, n = 3; P = 0.0115, paired t test).

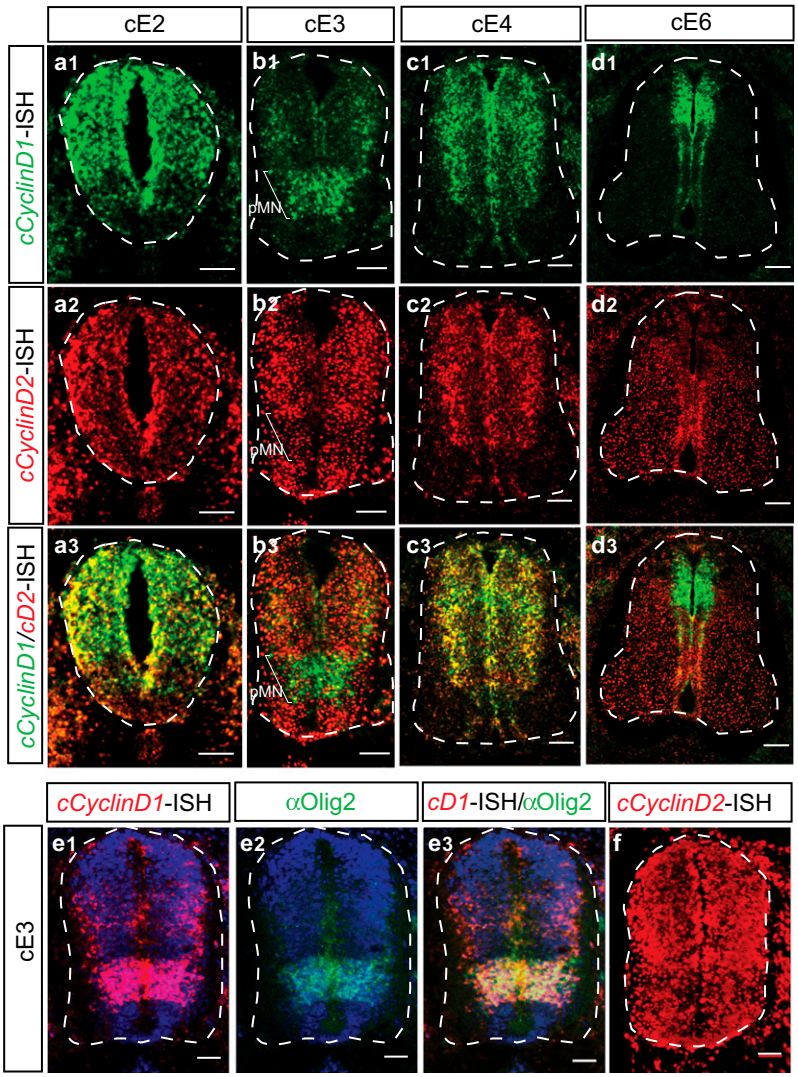

Fig. S3. Cyclin D1 expression correlates with neurogenesis in the chick spinal cord. (*A–D*) To examine the pattern of expression of Cyclin Ds throughout chick spinal cord neurogenesis, we performed double-FISH experiments. (*E* and *F*) To confirm the pattern of expression in pMN, cD1 (e) and cD2 (f) FISH was coimmunostained for Olig2. At cE2, cD1 and cD2 expression is uniform and overlapping (a1–a3). By cE3, the stage at which most MN production occurs, cD1 is highly expressed in pMN domain (b1–b3), as confirmed by coimmunostaining for Olig2 (e1–e3). Conversely, the pMN domain expresses a relatively low level of cD2. At later stages, cE4 and cE6, cD1 expression is high in the dorsal spinal cord, whereas cD2 appears restricted to a ventral position (c1–d3). The observed expression pattern of Cyclin D1 and D2 in the chick is highly reminiscent of their pattern of expression in the developing mouse spinal cord. In particular, at cE3, a stage comparable to mouse E9.5–E10.5, there was a striking colocalization of cD1 mRNA and Olig2 in the pMN domain, whereas cD2 mRNA expression was relatively weak within pMN but otherwise distributed uniformly throughout the neuroepithelium, as described previously (1). At later stages, cD1 mRNA became progressively restricted to the dorsal VZ (d1), as in the mouse.

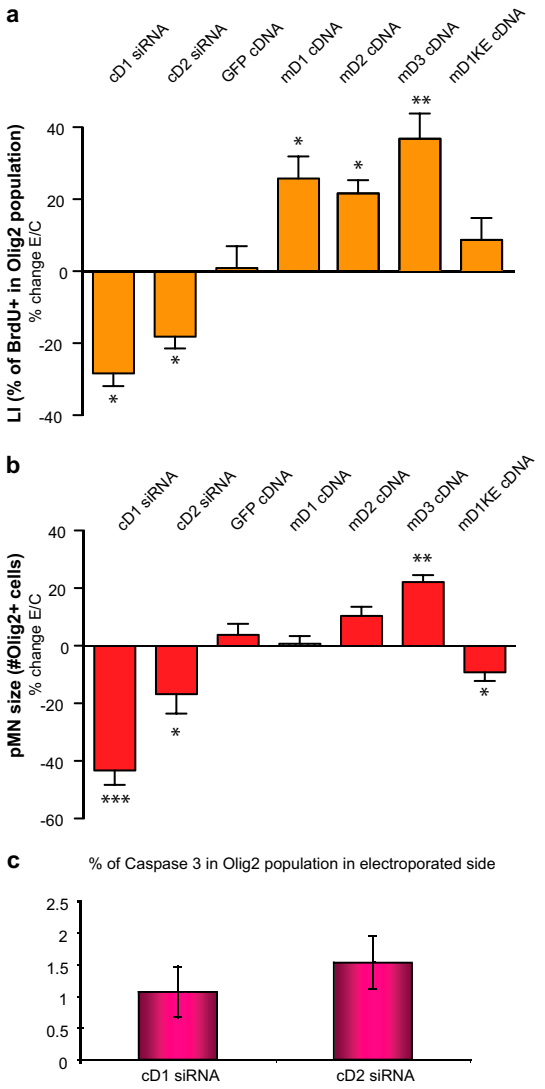

Fig. S4. Impact of acute manipulation of Cyclin Ds on proliferation and apoptosis. Modulation of Cyclin D expression is expected to modify the proliferation of progenitor cells. We monitored cell cycle kinetics and size of the pool of precursors to assess the functionality of our constructs in vivo. (*A*) The LI quantifies the percentage of Olig2$^+$ cells marked by BrdU. Values represent the percent change in BrdU$^+$/Olig2$^+$ cells on the electroporated side relative to the controlateral (nonelectroporated) side × 100%. Electroporation was performed at cE2 and analysis was done at cE4. Data represent mean ± SEM of between four and eight sections from three to six embryos, from *t* tests performed between the control GFP electroporation and each condition. shRNAs targeting cDs significantly decreased the LI, whereas overexpression of the three mD cDNAs significantly increased it. In contrast, overexpression of the mutant KE mouse Cyclin D1 cDNA (cDNA mD1KE) did not significantly influence proliferation, as expected. (*B*) Quantification of the number of cE4 Olig2$^+$ cells after cE2 electroporation. Values are the percent change in the number of Olig2$^+$ cells on the electroporated side relative to the controlateral (nonelectroporated) side × 100%. Data represent mean ± SEM of between four and eight sections from four to seven embryos, from *t* tests performed between each condition and the control GFP electroporation. Down-regulation of cDs significantly decreased the size of the pMN domain, whereas only the RCAS construct coding for mouse Cyclin D3 cDNA (cDNA mD3) significantly increased it. Overexpression of mutant KE mouse Cyclin D1 cDNA (cDNA mD1KE) significantly decreases the size of the pMN domain. (*C*) Quantification of the percentage of activated caspase-3$^+$ nuclei in Olig2$^+$ cells as a read out of apoptosis. No activated caspase-3 staining was found after electroporation of chick spinal cord at cE2 and analyses at cE4 and cE5, with the exception of electroporation of RCAS constructs containing a shRNA targeting cDs at cE4. shRNA constructs trigger marginal activation (~1% of Olig2$^+$ cells) of apoptosis as presented here, explained by shRNA overexpression toxicity.

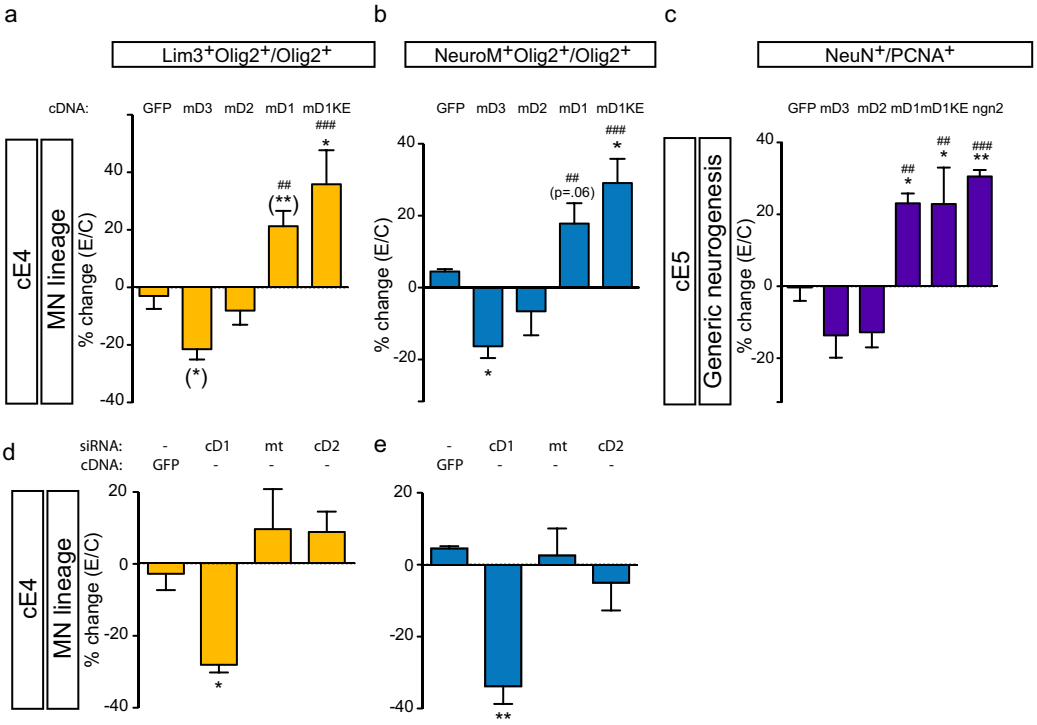

Fig. S5. Impact of Cyclin D1 overexpression on neurogenesis. (*A* and *B*) Quantification of the percentage of cE4 Olig2$^+$ cells expressing Lim3 (*A*) and NeuroM (*B*) after cE2 electroporations. Values represent the percent change in the proportion of marker-positive cells on the electroporated side relative to the controlateral (nonelectroporated) side × 100%. Data represent mean ± SEM of six to eight sections from four to seven embryos. One-way ANOVA statistical analysis shows significant differences between conditions (Lim 3, $P < 0.0001$; NeuroM, $P = 0.0001$): electroporation of GFP, mD1, mD2, mD3, and mD1KE. A Newman–Keuls posttest comparison found that only mD1KE significantly increased the percentage of Lim3$^+$ cells compared with GFP control (*A*, *); however, both mD1 and mD3 showed significant differences from the GFP by the *t* test (*A*, * between brackets). Both mD1 and mD1KE were significantly different from mD3 by a Newman–Keuls posttest comparison (*A*, #). Newman–Keuls posttest comparisons indicated that mD3 and mD1KE, but not mD1 or mD2, had a significant impact on the percentage of NeuroM$^+$ cells compared with GFP (*B*, *). All constructs but mD2 were significantly different from mD3 by the Newman–Keuls posttest (*B*, #). (*C*) Quantification of the ratio between the number of NeuN$^+$ and PCNA$^+$ cells in the cE5 spinal cord after electroporation at cE2. Values represent the percent change in the ratio on the electroporated side relative to the controlateral (nonelectroporated) side × 100%. Data represent the mean ± SEM of three sections from three embryos. One-way ANOVA statistical analysis shows significant differences between conditions ($P < 0.0001$): electroporation of GFP, mD1, mD2, mD3, mD1KE, and ngn2. Newman–Keuls posttest comparisons show significant differences, as indicated, when run against either GFP (*) or mD3 (#). (*D* and *E*) Quantification of the percentage of cE4 Olig2$^+$ cells expressing Lim3 (*D*) and NeuroM (*E*) after cE2 electroporation of the indicated constructs. Values represent the percent change in the proportion of marker-positive cells on the electroporated side relative to the controlateral (nonelectroporated) side × 100%. Data represent the mean ± SEM of six to eight sections from four to seven embryos. One-way ANOVA statistical analysis shows significant differences between conditions (Lim 3: $P = 0.0007$; NeuroM: $P = 0.0011$): electroporation of GFP, siRNA against cD1 (iD1), mutant siRNA against cD1 (mt), and siRNA against cD2 (iD2). Newman–Keuls posttest comparisons were performed. The data in *D* and *E* are from the same set of experiment as presented in Fig. 2 *A* and *B* and reproduced here for ease of comparison.

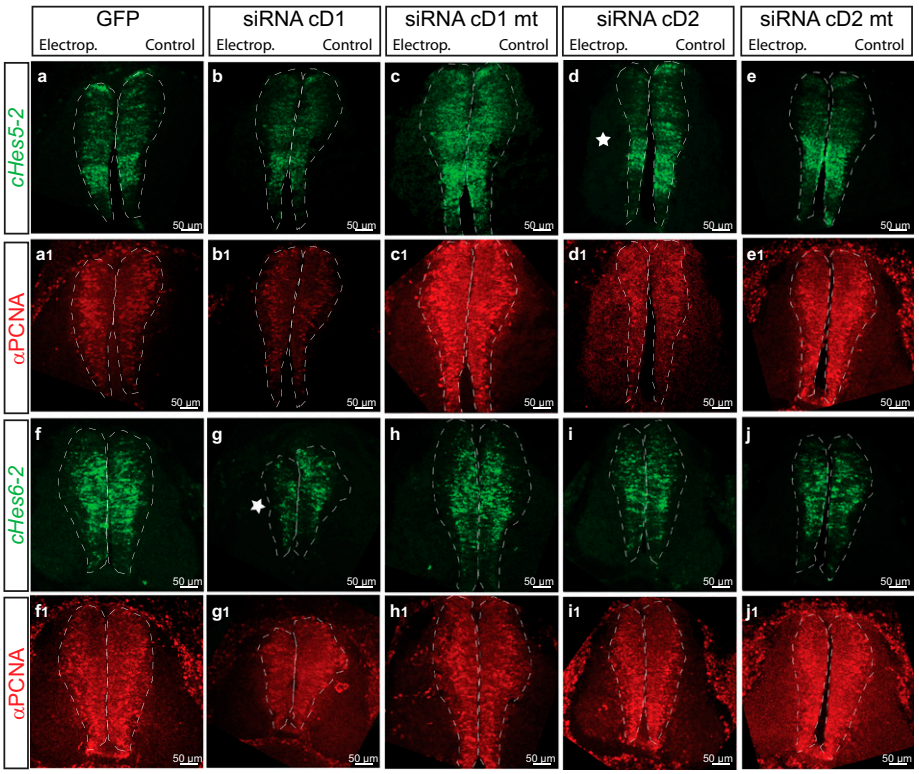

Fig. S6. Genetic interactions between Cyclin Ds and Notch signaling components. FISH for chick *Hes5-2* (*A–E*) or chick *Hes6-2* (*F–J*) combined with immunolabeling of PCNA on E5 spinal cord (a1–j1). Dashed lines delineate the VZ, marked by PCNA expression. Asterisks in *D* and *G* indicate reductions in *Hes5-2* and *Hes6-2* mRNAs caused by knockdown of cD2 and cD1, respectively. The GFP, siRNA cD1, and siRNA cD2 data presented here are the same as those shown in Fig. 3, and are reproduced for ease of comparison.

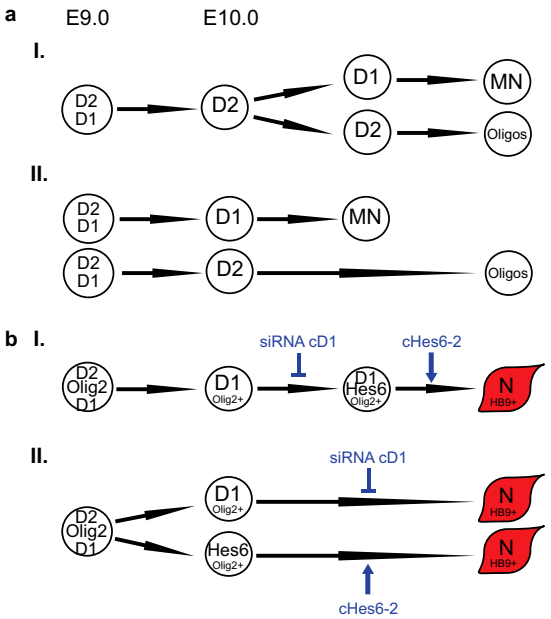

Fig. S7. Cyclin D1 promotes neurogenesis through a genetic pathway involving Hes genes. Additional alternative models to Fig. 4*D* are presented here. (*A*) Whereas Cyclin D1 and D2 highly overlap in the E9.5 pMN domain, only a minority of E10.0 Olig2$^+$ precursors coexpress them. Such active segregation could reflect either a sequential role for each Cyclin D with the MN lineage (I) or reveal the presence of distinct neurogenic and nonneurogenic populations within the pMN domain (II). (*B*) Models to explain genetic epistasis between Cyclin D1 and Hes6. (I) Cyclin D1 and Hes6 are sequentially expressed within the same lineage. Direct coexpression of Cyclin D1 and Hes6 has not yet been demonstrated, but is supported by indirect evidence (see the second part of *Discussion*). Rescue of the cD1 knockdown phenotype (siRNA cD1) by cHes6-2 in this model occurs via molecular compensation, reflecting either the normal pathway through which Cyclin D1 acts to promote neurogenesis, or a bypass effect of Hes6-2 overexpression. (II) Cyclin D1 and Hes6 are expressed in separate lineages. Rescue of in this model occurs by cellular compensation.

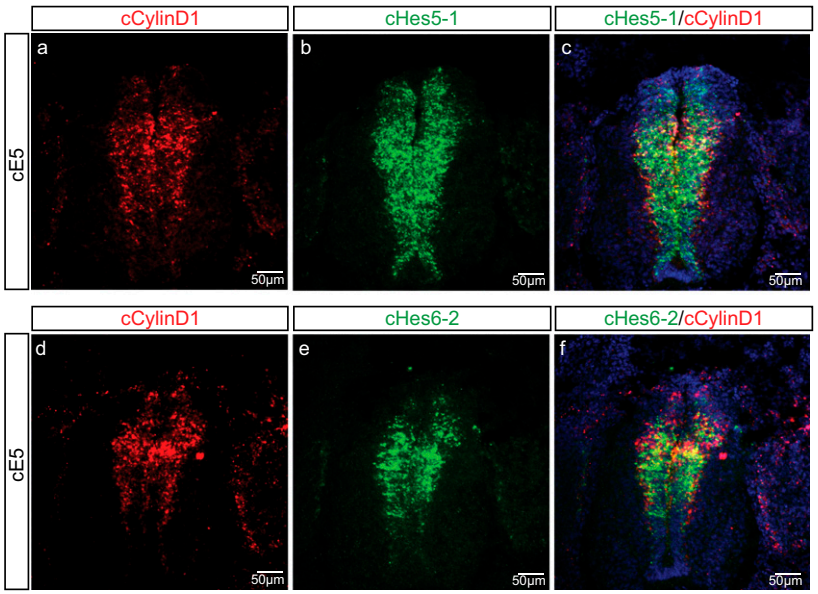

Fig. S8. cD1 expression correlates with cHes6-2. (*A*–*C*) Double-FISH for cD1 (*A*) and cHes5-1 (*B*) and overlay pictures (*C*) on cE5 chick spinal cord sections. (*D*–*F*) Double-FISH for cD1 (*D*) and cHes6-2 (*E*) and overlay pictures (*F*) on cE5 chick spinal cord sections. We performed double-FISH to compare expression of cD1 and cHes in the cE5 developing spinal cord. Whereas cHes5-2 is evenly expressed in the VZ (*B*), cD1 (*A* and *D*) and cHes6-2 (*E*) are expressed more greatly higher in the dorsal part of the VZ and in the outer ridge in the ventral part. Their expressions overlap significantly (*F*).